



Published in final edited form as:

*Eur Polym J.* 2015 August 1; 69: 532–539. doi:10.1016/j.eurpolymj.2015.01.043.

## Dual pH- and Temperature-Responsive Protein Nanoparticles

Nicholas M. Matsumoto<sup>a</sup>, George W. Buchman<sup>b</sup>, Leonard H. Rome<sup>c</sup>, and Heather D. Maynard<sup>\*,a</sup>

<sup>a</sup>Department of Chemistry and Biochemistry and California Nanosystems Institute, 607 Charles E. Young Drive East, University of California, Los Angeles, CA 90095-1569

<sup>b</sup>Paragon Bioservices, Inc., 801 W. Baltimore Street, Suite 401, Baltimore, MD 21201

<sup>c</sup>Department of Biological Chemistry, David Geffen School of Medicine and California Nanosystems Institute, University of California, Los Angeles, CA 90095

### Abstract

Multiply responsive protein nanoparticles are interesting for a variety of applications. Herein, we describe the synthesis of a vault nanoparticle that responds to both temperature and pH. Specifically, poly(*N*-isopropylacrylamide-*co*-acrylic acid) with a pyridyl disulfide end group was prepared by reversible addition-fragmentation chain transfer (RAFT) polymerization. The polymer had a lower critical solution temperature (LCST) of 31.9 °C at pH 5, 44.0 °C at pH 6 and above 60 °C at pH 7. The polymer was conjugated to human major vault protein (hMVP), and the resulting nanoparticle was analyzed by UV-Vis, dynamic light scattering (DLS) and electron microscopy. The data demonstrated that poly(*N*-isopropylacrylamide-*co*-acrylic acid)-vault conjugate did not respond to temperatures below 60 °C at pH 7, while the nanoparticles reversibly aggregated at pH 6. Furthermore, it was shown that the vault nanoparticle structure remained intact for at least three heat and cooling cycles. Thus, these dually responsive nanoparticles may serve as a platform for drug delivery and other applications.

### Keywords

Multiply responsive; vault; nanoparticle; conjugate

## 1. Introduction

The development of stimuli-responsive nanoparticles is at the forefront of research in the diagnosis and treatment of tumors.<sup>1–5</sup> There have been numerous reports of nanoparticles engineered to respond to external stimuli such as temperature,<sup>6–8</sup> pH,<sup>9–11</sup> light,<sup>12</sup> magnetic field,<sup>13, 14</sup> and reducing conditions.<sup>15, 16</sup> Furthermore, therapeutic nanoparticles have been developed that respond to two or more of these stimuli.<sup>17–24</sup> In one example, Li and coworkers reported the development of doxorubicin loaded polymer nanoparticles and

\*Telephone: +1 310 267 5162; maynard@chem.ucla.edu.

**Publisher's Disclaimer:** This is a PDF file of an unedited manuscript that has been accepted for publication. As a service to our customers we are providing this early version of the manuscript. The manuscript will undergo copyediting, typesetting, and review of the resulting proof before it is published in its final citable form. Please note that during the production process errors may be discovered which could affect the content, and all legal disclaimers that apply to the journal pertain.

polymersomes, composed of a block copolymer containing segments of poly(ethylene oxide) and poly(*trans*-*N*-(2-ethoxy-1,3-dioxan-5-yl) acrylamide), which assemble at physiological temperatures and disassemble in acidic conditions.<sup>23</sup> Such acid-sensitive nanoparticles may be useful for applications in intracellular drug delivery due to acidic conditions found in endosomes and lysosomes. To date, all of the previously reported multiply stimuli responsive nanoparticles have been prepared by synthetic means, through the use of synthetic polymers and inorganic materials.

Naturally occurring protein cages, such as virus capsids, ferritin, and vault nanocapsules, can serve as scaffold for complex hybrid protein-polymer nanoparticles. Protein cages offer precise architectures, which can be genetically engineered and synthetically modified.<sup>25–29</sup> We, and others, have developed functionalized protein cages by modification with synthetic polymers.<sup>28–39</sup> For example, Xi and coworkers have modified ferritin with cell-binding RGD peptides and demonstrated the encapsulation of doxorubicin within these ferritin nanoparticles. These nanoparticles were shown to inhibit tumor growth in mouse models.<sup>40</sup> We have previously reported the preparation of vault-poly(*N*-isopropylacrylamide) (pNIPAAm) conjugates, which were shown to undergo a reversible thermally triggered aggregation at 35.9 °C.<sup>38</sup> Vault nanoparticles, first reported by Kedersha and Rome in 1986, are natural ribonucleoprotein particles weighing 13 MDa and measuring 45 × 45 × 75 nm in dimension, with an interior measuring 5 × 10<sup>7</sup> Å<sup>3</sup>.<sup>41–45</sup> Vaults are non-immunogenic, and are present in most eukaryotes, including humans.<sup>42</sup> Recombinant vaults are hollow protein shells, each composed of 78 copies of a single ~100 kDa protein called major vault protein or MVP. These stable particles are currently being pursued as templates for the development of drug delivery vehicles. Vaults have been engineered to target specific cell types and have been modified to encapsulate hydrophobic drugs.<sup>46,47, 48</sup> Herein, we report the development of dual pH- and temperature-responsive vault nanoparticles. These multiply responsive vault nanoparticles have been prepared through the conjugation of poly(*N*-isopropylacrylamide-*co*-acrylic acid) (pNIPAAm-*co*-AA) to human recombinant vaults (hMVP vaults). Compared to pNIPAAm, which has an LCST of approximately 32 °C, pNIPAAm-*co*-AA undergoes much higher LCST transitions in basic conditions and much lower LCST transitions in acidic conditions.<sup>49, 50</sup> This is due to the presence of the AA monomer units, which are deprotonated in basic and neutral conditions making the copolymer more soluble in water. In acidic conditions the AA monomer units are protonated, which makes the copolymer more hydrophobic. Thus, we envisioned that this polymer would provide dually responsive nanoparticles when conjugated to the vault.

## 2. Results and Discussion

Our approach to developing a pH and temperature responsive vault nanoparticle is based on the conjugation of pNIPAAm-*co*-AA to human vaults. RAFT polymerization was used for the preparation of these polymers due to the precise level of control over polymer molecular weight and narrow molecular weight distribution afforded by this technique. A cysteine reactive pNIPAAm-*co*-AA was synthesized *via* RAFT copolymerization of NIPAAm and AA in the presence of a pyridyl disulfide trithiocarbonate CTA **1** with AIBN (NIPAAm:AA:CTA:AIBN, 124:6:1:0.1) in DMF at 80 °C (Scheme 1). The polymerization was stopped after 1 h at 78% NIPAAm conversion and 88% AA conversion by <sup>1</sup>H NMR

spectroscopy. The crude polymerization mixture was purified by extensive dialysis against MeOH to yield **polymer 1**. The number-average molecular weight ( $M_n$ ) was determined by  $^1\text{H}$  NMR to be 14.1 kDa. Analysis of the polymer by gel permeation chromatography (GPC) gave a similar  $M_n$  (GPC) of 14.2 kDa. The molecular weight dispersity was 1.21; however this value may be an under estimation because the polymer elutes close to the GPC solvent peak. The overall monomer composition of **polymer 1** was 94.9 % NIPAAm and 5.1 % AA, calculated from the percent conversions of NIPAAm and AA.

In previous studies, we found the RAFT trithiocarbonate endgroup to non-specifically react to thiols present on recombinant rat vaults. The trithiocarbonate endgroup of **polymer 1** was therefore transformed into a non-reactive isobutyronitrile group by radical exchange with AIBN (Scheme 2).<sup>51</sup> After extensive dialysis against MeOH, **polymer 2** was obtained. Complete removal of the trithiocarbonate endgroup was determined by the disappearance of the 305 nm trithiocarbonate absorption by UV-Vis. Endgroup analysis by  $^1\text{H}$ -NMR revealed a  $M_n$  (NMR) of 14.1 kDa and by GPC an  $M_n$ (GPC) of 14.2 kDa and of 1.21. Thus, radical exchange with AIBN did not significantly alter the polymer molecular weight and dispersity.

The pH and temperature dependent thermal aggregation of **polymer 2** was evaluated by UV-Vis turbidity studies at pH 5.0, 6.0, and 7.0 (50 mM PB) (Figure 1). At pH 5.0 the lower critical solution temperature (LCST) was determined to be 31.9 °C. At pH 6.0 the LCST was determined to be 44.0 °C. At pH 7.0 there was no measureable LCST until at least 60 °C. As expected, the LCST of **polymer 2** increased as the pH level was increased, and the polymer became more hydrophilic.

**Polymer 2** was conjugated to human MVP (hMVP) vaults by incubation with the purified particles at a ratio of 100: 1 polymer : vaults to yield **conjugate 1** (Scheme 3). The conjugate was analyzed by SDS-PAGE, to observe a shift in molecular weight of the hMVP-pNIPAAm-co-AA conjugates as compared to unmodified hMVP. Conjugation is apparent in the SDS-PAGE (Figure 2). Under non-reducing conditions, SDS-PAGE stained with coomassie blue shows a shift to a higher molecular weight of the conjugate (Figure 2, Lane 5) when compared to the hMVP (~100 kDa) (Figure 2, Lane 4). The non-reduced conjugate appears (Figure 2, Lane 5) appears much fainter than the hMVP (Figure 2, Lane 4), which is a discreet band. This is because the conjugate band is spread out due to multiple polymer attachments per protein. This data shows that conjugation was highly efficient, as there is no free hMVP protein visible in the SDS-PAGE. Under reducing conditions with dithiothreitol (DTT), SDS-PAGE stained with coomassie blue shows no difference in molecular weight of the conjugate compared to the unmodified hMVP due to the disulfide bond between the polymer and hMVP of the conjugate being reduced (Figure 2, Lane 3). This provides better evidence that the polymer conjugate was made. The exact polymer conjugation sites on the vault structure are unknown. However, due to the presence of free cysteine residues on the vault interior and exterior, we expect that there is polymer conjugated on both the vault interior and exterior. We have previously conducted a number of experiments to determine precise conjugation sites of polymer attachment to vaults, but these attempts were unsuccessful.<sup>38</sup>

The pH and temperature responsive properties of the pNIPAAm-*co*-AA-vault conjugates were investigated by UV-Vis turbidity measurements in 20 mM 2-(*N*-morpholino)ethanesulfonic acid (MES) at pH 6.0 and 7.0 (Figure 3 C–D) and compared to unmodified vaults at those pHs (Figure 3 A–B). At pH 7.0 the conjugate did not display LCST behavior below 60 °C, similar to the polymer itself (Figure 3.C). However, at Ph 6.0 the conjugate aggregated upon heating and was determined to have an LCST of 41.8 °C (Figure 3.D). This is slightly lower than the LCST of the polymer itself at that pH (44.0 °C). Typically, conjugation of a protein to pNIPAAm increases the temperature slightly. The discrepancy is likely do to inaccurate measurement of the LCST of the conjugate. At higher temperatures (>45 °C) in pH 6.0 buffer, the conjugate precipitated from solution to form macroscopic aggregates; so the curve did not plateau confounding determination of the LCST, which is defined as 10% absorbance change. Unmodified hMVP vaults did not exhibit LCST behavior at pH 7.0 or 6.0, although at the latter pH close to 60 °C, the vault itself started to precipitate (Figure 3. A–B).

The pH and temperature dependent aggregation of the pNIPAAm-*co*-AA vault conjugates were next investigated by dynamic light scattering (DLS) in 20 mM MES at pH 6.0 and 7.0. At pH 7.0, the conjugate remained the same diameter at 25 °C ( $39.7 \pm 13.7$  nm) and 45 °C ( $40.4 \pm 12.7$  nm). However, when the conjugate was in pH 6.0 buffer, there was a shift in conjugate size from  $41.3 \pm 11.6$  nm at 25 °C to large aggregates (~300 nm) at 45 °C. The aggregation was reversible, and the conjugate returned to  $39.3 \pm 13.0$  nm when cooled to 25 °C. At both pH 6.0 and 7.0 there was almost no change in the unmodified vault size when the temperature was elevated from 25 to 45 °C. Together, the UV-Vis turbidity studies, as well as the DLS size measurements indicate that the polymer is conjugated to the hMVP vaults and that pH- and temperature-responsiveness is due to the conjugated polymer. Unmodified vaults remain intact and in solution when heated close to 60 °C, suggesting that the pH- and temperature-responsiveness of the conjugate is solely due to the conjugated polymer.

To confirm the reversibility of the aggregation and ascertain the integrity of the vault structure after temperature cycles at various pH's, hMVP vaults and the pNIPAAm-*co*-AA conjugates were visualized by electron microscopy before and after heating above 45 °C, which is above the LCST of the conjugate at pH 6.0 (Figure 4.5). At pH 6.0 (20 mM MES) the vault conjugate was found to remain intact throughout the thermally triggered aggregation process. At pH 6.5 (20 mM MES), the hMVP vaults, as well as the conjugate, were not damaged by heating. Furthermore, the conjugates were able to withstand three heating cycles without damaging the vault structure (Figure 4.5.H–I).

Together this data demonstrates the development of a dual pH- and temperature-responsive vault nanoparticle. All experiments with this vault conjugate were conducted in 20 mM MES buffer, however it may be possible to further control aggregation behavior by altering the salt concentration of the buffer.<sup>52</sup> These dual-responsive vault-pNIPAAm-*co*-AA conjugates can be tuned to specific LCST values by the incorporation of more or less AA monomer units to the polymer. This suggests that we will be able to tune the LCSTs of future vault-pNIPAAm-*co*-AA conjugates for specific applications such as intracellular drug delivery, where endosome and lysosome pH levels are known to be 5–6 and 4–5,

respectively.<sup>53</sup> Furthermore, this technology may be applicable to solid tumor delivery as some tumors are known to have pH levels as low as 5.7.<sup>54</sup>

As previously demonstrated with the vault-pNIPAAm conjugates,<sup>38</sup> conjugation of pNIPAAm-co-AA does not interfere with the vault structure, which is important for potential future applications of this pH- and temperature-responsive vault conjugate. Hydrophobic molecules, chemotherapeutics, proteins, and inorganic nanoparticles have all been packaged into the vault interior.<sup>46</sup> These vault loading techniques should be compatible with polymer conjugation to the vault, enabling multiple-responsive loaded vault conjugates.

### 3. Experimental

#### 3.1. Materials

Chemicals were purchased from Sigma-Aldrich, Fisher Scientific, and Acros. AIBN was recrystallized twice from acetone. NIPAAm was recrystallized twice from hexanes. The pyridyl disulfide trithiocarbonate CTA **1** was prepared according to previous literature.<sup>55</sup>

#### 3.2. Analytical Techniques

NMR spectra were obtained on Bruker 500 MHz DRX spectrometer. Proton NMR spectra were acquired with a relaxation delay of 30 sec for all polymers. UV-Vis spectra were obtained on a Biomate 5 Thermo Spectronic UV-Vis spectrometer and a Hewlett-Packard HP8453 diode-array UV-Vis spectrophotometer with Peltier temperature control spectrometer with quartz cells. Gel Permeation Chromatography (GPC) was conducted on a Shimadzu HPLC system equipped with a refractive index detector (RID-10A), one Polymer Laboratories PLgel guard column, and two Polymer Laboratories PLgel 5  $\mu$ m mixed D columns. LiBr (0.1 M) in DMF at 40 °C was used as an eluent (flow rate: 0.80 mL/min). Calibration was performed using near-monodisperse PMMA standards from Polymer Laboratories. SDS-PAGE was performed using Bio-Rad Any kD Mini-PROTEAN-TGX gels. Dynamic light scattering (DLS) was conducted on a Malvern Zetasizer Nano-S. TEM was conducted on a JEOL JEM1200-EX transmission electron microscope. Images were taken using a Gatan BioScan 600W 1x1K digital camera and Digital Micrograph acquisition software.

#### 3.3. Methods

**Copolymerization of NIPAAm and AA in the presence of pyridyl disulfide CTA to afford  $\alpha$ -pyridyl disulfide pNIPAAm-co-AA (polymer **1**)**—The pyridyl disulfide CTA **1** (45 mg, 0.11 mmol), NIPAAm (1.6 g, 14.1 mmol), AA (47  $\mu$ L, 0.62 mmol), and AIBN (1.9 mg, 0.011 mmol), were added to a Schlenk tube containing a magnetic stir bar. DMF (2.28 mL) was added to dissolve the solids. Freeze-pump-thaw cycles were repeated four times and the reaction was performed at 80 °C in an oil bath. The reaction was stopped after 1 h at 78% NIPAAm conversion and 88% AA conversion by cooling with liquid nitrogen and exposing the reaction to atmosphere. **Polymer 1** was purified by dialyzing against MeOH (MWCO 3,500 g/mol). <sup>1</sup>H NMR (500 MHz, MeOD)  $\delta$ : 8.39 (m, Py), 8.18–7.25 (NH, pNIPAAm), 7.214 (m, Py), 7.26 (m), 4.27 (m), 4.12–3.73 (CH, pNIPAAm), 3.06 (s), 2.35–1.80 (CH<sub>2</sub>, pNIPAAm), 1.79–1.45 (CH<sub>2</sub>, pNIPAAm), 1.25–0.92 (NCH<sub>3</sub>,

pNIPAAm). The signals corresponding to AA are unidentifiable by  $^1\text{H}$  NMR of the purified polymer. The incorporation of AA was calculated from the % conversion of the AA in the crude  $^1\text{H}$  NMR of the polymer at 1 h.  $M_n$  by  $^1\text{H}$  NMR was 14,100 g/mol (targeted 12,000 g/mol).  $M_n$ (GPC) was 14,200 g/mol and the  $\text{PDI}$  was 1.21.

**Trithiocarbonate endgroup removal by radical exchange with AIBN to yield polymer 2—Polymer 1** (112 mg, 0.008 mmol) and AIBN (26.3 mg, 0.160 mmol) were added to a Schlenk tube containing a magnetic stir bar with DMF (1.56 mL). Freeze-pump-thaw cycles were repeated three times, and polymerization was then initiated by submerging the Schlenk tube in an oil bath at 80 °C. **Polymer 2** was obtained after dialyzing the crude reaction mixture against MeOH (MWCO 3,500 g/mol). Complete removal of the trithiocarbonate end group was observed by monitoring the UV-Vis absorption at 305 nm.  $^1\text{H}$  NMR (500 MHz, MeOD)  $\delta$ : 8.39 (m, Py), 8.19–7.26 (NH, pNIPAAm), 7.23 (m, Py), 7.26 (d), 4.28 (m), 4.10–3.76 (CH, pNIPAAm), 3.06 (s), 2.48–1.79 (CH<sub>2</sub>, pNIPAAm), 1.79–1.44 (CH<sub>2</sub>, pNIPAAm), 1.32–0.92 (NCH<sub>3</sub>, pNIPAAm). The signals corresponding to AA are unidentifiable by  $^1\text{H}$  NMR.  $M_n$  by  $^1\text{H}$  NMR was 14,100 g/mol (targeted 12,000 g/mol).  $M_n$ (GPC) was 14,200 g/mol and the  $\text{PDI}$  was 1.25.

**Expression and Purification of hMVP Vaults**—Vaults were isolated from insect larvae produced by Chesapeake PERL, Inc. using its PERLXpress system, a protein expression platform that combines recombinant baculovirus technology with mass oral infection of synchronous *Trichoplusia ni* larvae. Larvae were infected with a recombinant baculovirus encoding the human MVP cDNA, which included a CP peptide at the MVP N-terminus. This peptide has been shown to stabilize recombinant vaults.<sup>56</sup> After 96 hours larvae were harvested and frozen, and later homogenized in a pH 7.4 buffer (50 mM Tris, 1 M NaCl, 1 mM MgCl<sub>2</sub>) containing protease inhibitors. The homogenate was clarified by low speed centrifugation for 30 min and the vaults precipitated with 3% PEG6000. The pellet was collected after a low speed centrifugation, washed and solubilized by re-suspension in 30 mM Tris, 1 mM MgCl<sub>2</sub>, pH 7.4 with protease inhibitors and 0.05% Triton X-100 was added after filtration through a 0.22 micron filter unit (Millipak 40). The sample was then fractionated on a Fractogel® EMD TMAE ion exchange column. We achieved ~99% purity after passage over this single column. A second polishing gel filtration chromatography column (Superdex 200) resulted in hMVP Vaults with an estimated purity >99%.

**pNIPAAm-co-AA conjugation to hMVP**—A pH 6.5 20 mM MES buffer was degassed by bubbling argon gas through the buffer for 30 min. hMVP (0.50 mg, 0.05  $\mu\text{mol}$ ) in 250  $\mu\text{L}$  buffer was treated with triscarboxylethylphosphine (TCEP) resin for 2 h at 4 °C, then filtered through a 0.22  $\mu\text{m}$  syringe filter. **Polymer 2** (6.20 mg, 5.00  $\mu\text{mol}$ ) was dissolved in 250  $\mu\text{L}$  of buffer. The filtered hMVP vault solution was added to the solution containing **polymer 2**. The reaction was incubated at 4 °C for 24 h before purification by ultrafiltration (MWCO 100,000 g/mol) to give the conjugate.

**LCST determination**—A solution of **polymer 2**, conjugate, or unmodified vault at a concentration of 1.0 mg mL<sup>-1</sup> in pH 5.0, 6.0, or 7.0 20 mM MES was placed in a 100  $\mu\text{L}$

quartz cuvette. The cuvette was placed in a Hewlett-Packard HP8453 diode-array UV-Vis spectrophotometer with Peltier temperature control. The following temperature program was used: temperature was elevated at  $0.5\text{ }^{\circ}\text{C min}^{-1}$  and held for 30 s prior to measuring the absorbance at 600 nm. The LCST was determined at 10% of the maximum absorbance.

**DLS size determination**—A solution of unmodified vault or conjugate at a concentration of  $1\text{ mg mL}^{-1}$  in pH 6.0 or 7.0 20 mM MES was placed in a 40  $\mu\text{L}$  disposable cuvette. The cuvette was placed in a Malvern Zetasizer Nano-S and heated to 25 or 45  $^{\circ}\text{C}$ . The temperature was allowed to equilibrate for three minutes before beginning the DLS measurement. Each measurement was repeated three times, sizes are reported as an average of three measurements.

**Preparation of the TEM sample**—A 40  $\mu\text{L}$  aliquot of a  $0.2\text{ }\mu\text{g }\mu\text{L}^{-1}$  solution of hMVP-vault-pNIPAAm conjugate in either pH 6.0, 6.5, or 7.0 (20 mM MES) was warmed to 45  $^{\circ}\text{C}$  incubated for 7 min then cooled to 4  $^{\circ}\text{C}$ . 20  $\mu\text{L}$  of the solution was then pipetted onto a parafilm-coated aluminum surface cooled to 4  $^{\circ}\text{C}$ . A carbon-coated EM grid was floated up-side down on the sample to allow the conjugate to adsorb to the grid surface. After 5 min, the grid was removed from the sample and blotted on filter paper to remove excess liquid. The grid was then floated up-side down in 500  $\mu\text{L}$  of a 1% uranyl acetate solution at the 4  $^{\circ}\text{C}$ . After 5 min, the grid was removed from the uranyl acetate solution and blotted on filter paper. TEM was then conducted on a JEOL JEM1200-EX transmission electron microscope.

## 4. Conclusions

Dual pH- and temperature- responsive vault nanoparticles have been prepared through the conjugation of pNIPAAm-*co*-AA to human vaults. This conjugate was shown to undergo a thermally triggered reversible aggregation at 41.8  $^{\circ}\text{C}$  in pH 6.0 buffer, while remaining stable in solution at pH 7.0. The dual-responsive properties of this conjugate in combination with reported vault loading strategies, may be useful for intracellular drug delivery and solid tumor drug delivery.

## Supplementary Material

Refer to Web version on PubMed Central for supplementary material.

## Acknowledgments

This work was funded by the National Institutes of Health (R21 CA 137506-01). N. M. Matsumoto thanks the National Science Foundation for a Graduate Research Fellowship (DGE-0707424) and UCLA for a Dissertation Year Fellowship. The authors acknowledge the use of instruments at the Electron Imaging Center for NanoMachines supported by NIH (1S10RR23057) and CNSI at UCLA.

## References

1. Peer D, et al. Nanocarriers as an emerging platform for cancer therapy. *Nat Nanotechnol.* 2007; 2:751–760. [PubMed: 18654426]
2. Ferrari M. Cancer nanotechnology: Opportunities and challenges. *Nat Rev Cancer.* 2005; 5:161–171. [PubMed: 15738981]

3. Brigger I, Dubernet C, Couvreur P. Nanoparticles in cancer therapy and diagnosis. *Adv Drug Deliv Rev.* 2002; 54:631–651. [PubMed: 12204596]
4. Davis ME, Chen Z, Shin DM. Nanoparticle therapeutics: an emerging treatment modality for cancer. *Nat Rev Drug Discov.* 2008; 7:771–782. [PubMed: 18758474]
5. Fonseca NA, Gregorio AC, Valerio-Fernandes A, Simoes S, Moreira JN. Bridging cancer biology and the patients' needs with nanotechnology-based approaches. *Cancer Treat Rev.* 2014; 40:626–635. [PubMed: 24613464]
6. Cammas S, et al. Thermo-responsive polymer nanoparticles with a core-shell micelle structure as site-specific drug carriers. *J Control Release.* 1997; 48:157–164.
7. Berndt I, Pedersen JS, Richtering W. Temperature-sensitive core-shell microgel particles with dense shell. *Angew Chem Int Ed.* 2006; 45:1737–1741.
8. Hellweg T, Dewhurst CD, Eimer W, Kratz K. PNIPAM-co-polystyrene core-shell microgels: Structure, swelling behavior, and crystallization. *Langmuir.* 2004; 20:4330–4335. [PubMed: 15969135]
9. Soppimath KS, Tan DCW, Yang YY. pH-triggered thermally responsive polymer core-shell nanoparticles for drug delivery. *Adv Mat.* 2005; 17:318–+.
10. Das M, Mardiyani S, Chan WCW, Kumacheva E. Biofunctionalized pH-responsive microgels for cancer cell targeting: Rational design. *Adv Mat.* 2006; 18:80–83.
11. Dupin D, Fujii S, Armes SP, Reeve P, Baxter SM. Efficient synthesis of sterically stabilized pH-responsive microgels of controllable particle diameter by emulsion polymerization. *Langmuir.* 2006; 22:3381–3387. [PubMed: 16548605]
12. Angelatos AS, Radt B, Caruso F. Light-responsive polyelectrolyte/gold nanoparticle microcapsules. *J Phys Chem B.* 2005; 109:3071–3076. [PubMed: 16851322]
13. Pankhurst QA, Connolly J, Jones SK, Dobson J. Applications of magnetic nanoparticles in biomedicine. *J Phys D Appl Phys.* 2003; 36:R167–R181.
14. Lu AH, Salabas EL, Schuth F. Magnetic nanoparticles: Synthesis, protection, functionalization, and application. *Angew Chem Int Ed.* 2007; 46:1222–1244.
15. Ryu JH, et al. Self-Cross-Linked Polymer Nanogels: A Versatile Nanoscopic Drug Delivery Platform. *J Am Chem Soc.* 2010; 132:17227–17235. [PubMed: 21077674]
16. Ryu JH, Jiwpanich S, Chacko R, Bickerton S, Thayumanavan S. Surface-Functionalizable Polymer Nanogels with Facile Hydrophobic Guest Encapsulation Capabilities. *J Am Chem Soc.* 2010; 132:8246–8247. [PubMed: 20504022]
17. Jaiswal MK, Pradhan A, Banerjee R, Bahadur D. Dual pH and Temperature Stimuli-Responsive Magnetic Nanohydrogels for Thermo-Chemotherapy. *J Nanosci Nanotechnol.* 2014; 14:4082–4089.
18. Hoare T, Pelton R. Highly pH and temperature responsive microgels functionalized with vinylacetic acid. *Macromolecules.* 2004; 37:2544–2550.
19. Kuckling D, Vo CD, Wohlrab SE. Preparation of nanogels with temperature-responsive core and pH-responsive arms by photo-cross-linking. *Langmuir.* 2002; 18:4263–4269.
20. Isojima T, Lattuada M, Vander Sande JB, Hatton TA. Reversible clustering of pH- and temperature-responsive Janus magnetic nanoparticles. *ACS Nano.* 2008; 2:1799–1806. [PubMed: 19206418]
21. Cheng R, Meng FH, Deng C, Klok HA, Zhong ZY. Dual and multi-stimuli responsive polymeric nanoparticles for programmed site-specific drug delivery. *Biomaterials.* 2013; 34:3647–3657. [PubMed: 23415642]
22. Kang SI, Na K, Bae YH. Physicochemical characteristics and doxorubicin-release behaviors of pH/temperature-sensitive polymeric nanoparticles. *Colloid Surface A.* 2003; 231:103–112.
23. Qiao ZY, et al. Polymersomes from Dual Responsive Block Copolymers: Drug Encapsulation by Heating and Acid-Triggered Release. *Biomacromolecules.* 2013; 14:1555–1563. [PubMed: 23570500]
24. Wang AN, et al. Temperature- and pH-responsive nanoparticles of biocompatible polyurethanes for doxorubicin delivery. *Int J Pharm.* 2013; 441:30–39. [PubMed: 23262421]



25. Douglas T, Young M. Virus particles as templates for materials synthesis. *Adv Mat.* 1999; 11:679–681.
26. Witus LS, Francis MB. Using Synthetically Modified Proteins to Make New Materials. *Acc Chem Res.* 2011; 44:774–783. [PubMed: 21812400]
27. Lee LA, Niu ZW, Wang Q. Viruses and Virus-Like Protein Assemblies-Chemically Programmable Nanoscale Building Blocks. *Nano Res.* 2009; 2:349–364.
28. Uchida M, et al. Biological containers: Protein cages as multifunctional nanoplatfoms. *Adv Mat.* 2007; 19:1025–1042.
29. Soto CM, Ratna BR. Virus hybrids as nanomaterials for biotechnology. *Curr Opin Biotech.* 2010; 21:426–438. [PubMed: 20688511]
30. MaHam A, Tang ZW, Wu H, Wang J, Lin YH. Protein-Based Nanomedicine Platforms for Drug Delivery. *Small.* 2009; 5:1706–1721. [PubMed: 19572330]
31. Manchester M, Singh P. Virus-based nanoparticles (VNPs): Platform technologies for diagnostic imaging. *Adv Drug Deliv Rev.* 2006; 58:1505–1522. [PubMed: 17118484]
32. Ma YJ, Nolte RJM, Cornelissen J. Virus-based nanocarriers for drug delivery. *Adv Drug Deliv Rev.* 2012; 64:811–825. [PubMed: 22285585]
33. Garcea RL, Gissmann L. Virus-like particles as vaccines and vessels for the delivery of small molecules. *Curr Opin Biotech.* 2004; 15:513–517. [PubMed: 15560977]
34. Nam KT, et al. Virus-Enabled Synthesis and Assembly of Nanowires for Lithium Ion Battery Electrodes. *Science.* 2006; 312:885–888. [PubMed: 16601154]
35. Jutz G, Boker A. Bionanoparticles as functional macromolecular building blocks – A new class of nanomaterials. *Polymer.* 2011; 52:211–232.
36. Steinmetz NF, Evans DJ. Utilisation of plant viruses in bionanotechnology. *Org Biomol Chem.* 2007; 5:2891–2902. [PubMed: 17728853]
37. Endo M, Fujitsuka M, Majima T. Porphyrin light-harvesting arrays constructed in the recombinant tobacco mosaic virus scaffold. *Chem-Eur J.* 2007; 13:8660–8666. [PubMed: 17849494]
38. Matsumoto NM, Prabhakaran P, Rome LH, Maynard HD. Smart Vaults: Thermally-Responsive Protein Nanocapsules. *ACS Nano.* 2013; 7:867–874. [PubMed: 23259767]
39. Lucon J, et al. Use of the interior cavity of the P22 capsid for site-specific initiation of atom-transfer radical polymerization with high-density cargo loading. *Nat Chem.* 2012; 4:781–788. [PubMed: 23000990]
40. Zhen ZP, et al. RGD-Modified Apoferritin Nanoparticles for Efficient Drug Delivery to Tumors. *ACS Nano.* 2013; 7:4830–4837. [PubMed: 23718215]
41. Kedersha NL, Rome LH. ISOLATION AND CHARACTERIZATION OF A NOVEL RIBONUCLEOPROTEIN PARTICLE – LARGE STRUCTURES CONTAIN A SINGLE SPECIES OF SMALL RNA. *J Cell Biol.* 1986; 103:699–709. [PubMed: 2943744]
42. Kedersha NL, Miquel MC, Bittner D, Rome LH. VAULTS .2. RIBONUCLEOPROTEIN STRUCTURES ARE HIGHLY CONSERVED AMONG HIGHER AND LOWER EUKARYOTES. *J Cell Biol.* 1990; 110:895–901. [PubMed: 1691193]
43. Suprenant KA. Vault ribonucleoprotein particles: Sarcophagi, gondolas, or safety deposit boxes? *Biochemistry.* 2002; 41:14447–14454. [PubMed: 12463742]
44. Kong LB, Siva AC, Rome LH, Stewart PL. Structure of the vault, a ubiquitous cellular component. *Structure.* 1999; 7:371–379. [PubMed: 10196123]
45. Kedersha NL, Heuser JE, Chugani DC, Rome LH. VAULTS .3. VAULT RIBONUCLEOPROTEIN-PARTICLES OPEN INTO FLOWER-LIKE STRUCTURES WITH OCTAGONAL SYMMETRY. *J Cell Biol.* 1991; 112:225–235. [PubMed: 1988458]
46. Rome LH, Kickhoefer VA. Development of the Vault Particle as a Platform Technology. *ACS Nano.* 2013; 7:889–902. [PubMed: 23267674]
47. Kickhoefer VA, et al. Targeting Vault Nanoparticles to Specific Cell Surface Receptors. *ACS Nano.* 2009; 3:27–36. [PubMed: 19206245]
48. Buehler DC, Toso DB, Kickhoefer VA, Zhou ZH, Rome LH. Vaults Engineered for Hydrophobic Drug Delivery. *Small.* 2011; 7:1432–1439. [PubMed: 21506266]

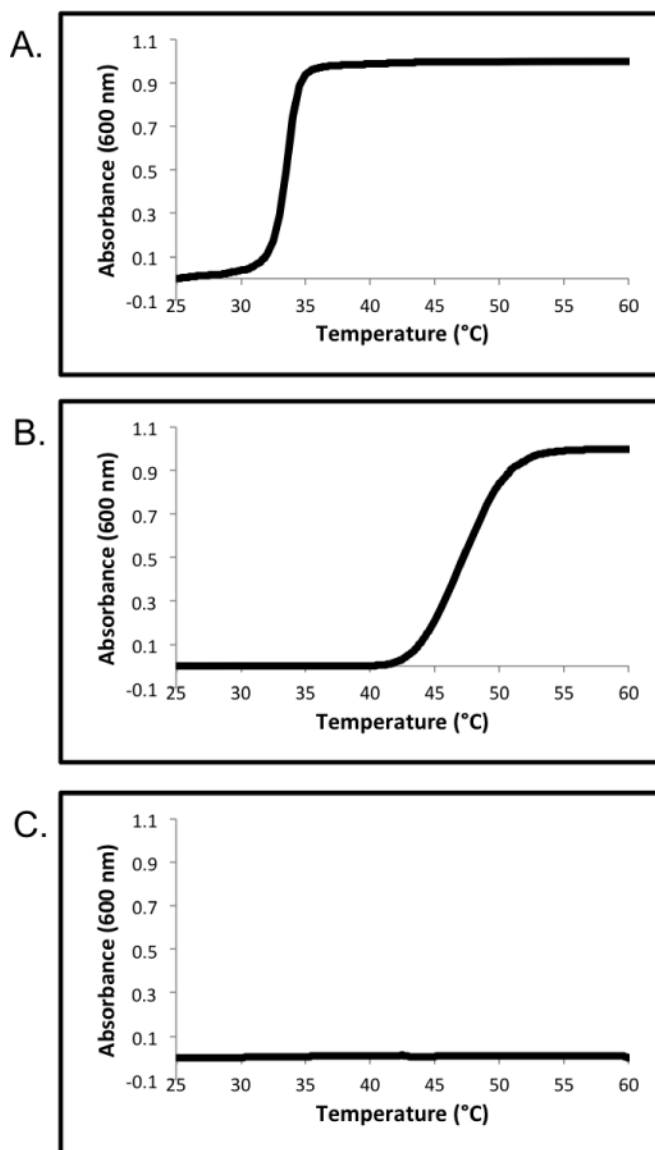
49. Chen G, Hoffman AS. Temperature-induced phase transition behaviors of random vs. graft copolymers of N-isopropylacrylamide and acrylic acid. *Macromol Rapid Commun.* 1995; 16:175–182.
50. Jones MS. Effect of pH on the lower critical solution temperatures of random copolymers of N-isopropylacrylamide and acrylic acid. *Eur Polym J.* 1999; 35:795–801.
51. Perrier S, Takolpuckdee P, Mars CA. Reversible addition-fragmentation chain transfer polymerization: End group modification for functionalized polymers and chain transfer agent recovery. *Macromolecules.* 2005; 38:2033–2036.
52. Yoo MK, Sung YK, Lee YM, Cho CS. Effect of polyelectrolyte on the lower critical solution temperature of poly(*N*-isopropyl acrylamide) in the poly(NIPAAm-*co*-acrylic acid) hydrogel. *Polymer.* 41:5713–5719.
53. Duncan R. DRUG POLYMER CONJUGATES – POTENTIAL FOR IMPROVED CHEMOTHERAPY. *Anti-Cancer Drug.* 1992; 3:175–210.
54. Soppimath KS, Tan DCW, Yang YY. pH-Triggered Thermally Responsive Polymer Core–Shell Nanoparticles for Drug Delivery. *Adv Mat.* 2005; 17:318–323.
55. Mancini RJ, Lee J, Maynard HD. Trehalose Glycopolymers for Stabilization of Protein Conjugates to Environmental Stressors. *J Am Chem Soc.* 2012; 134:8474–8479. [PubMed: 22519420]
56. Mikyas Y, et al. Cryoelectron microscopy imaging of recombinant and tissue derived vaults: Localization of the MVP N termini and VPARP. *Journal of Molecular Biology.* 2004; 344:91–105. [PubMed: 15504404]

### Highlights

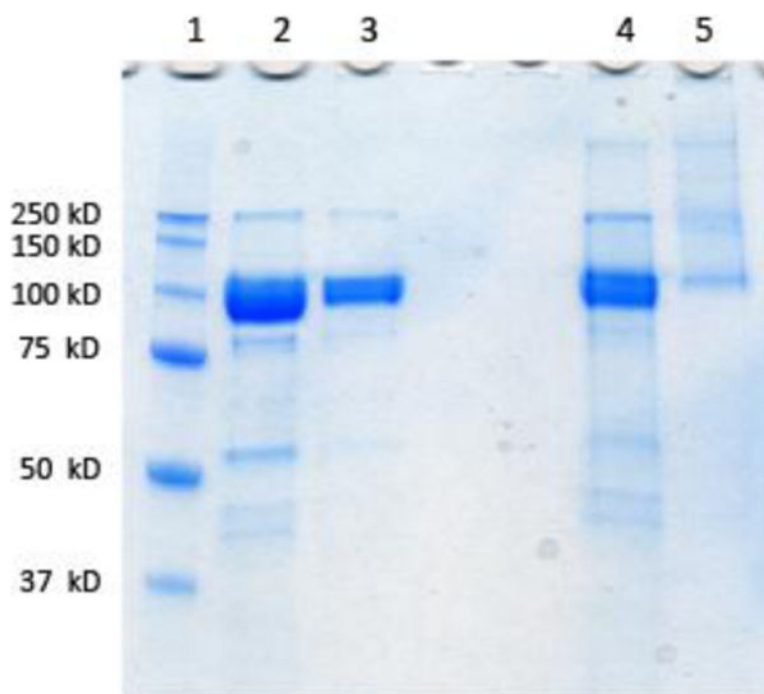
We describe dually-responsive vault-polymer biohybrid nanoparticles.

Poly(*N*-isopropylacrylamide-*co*-acrylic acid) was conjugated to human major vault protein.

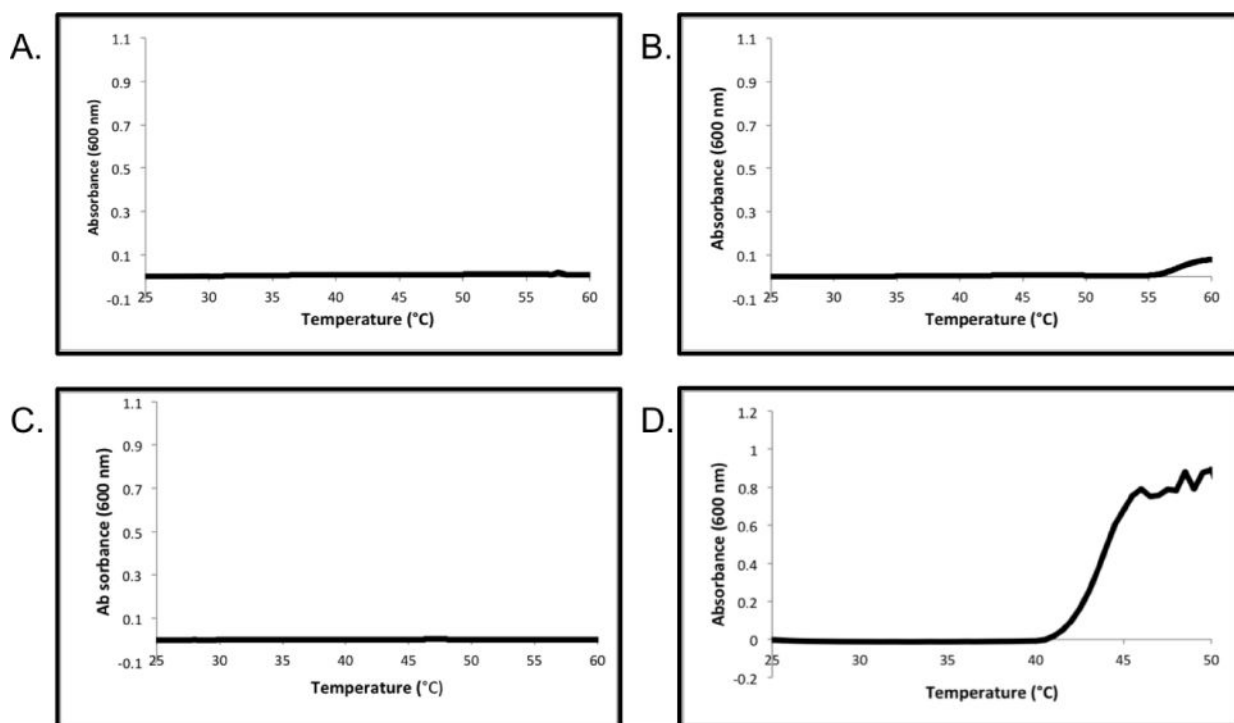
The smart vault reversibly aggregates depending on pH and temperature.



**Figure 1.** UV-Vis turbidity experiments of **polymer 2** in 50 mM PB at: (A) pH 5.0; (B) pH 6.0; (C) pH 7.0.

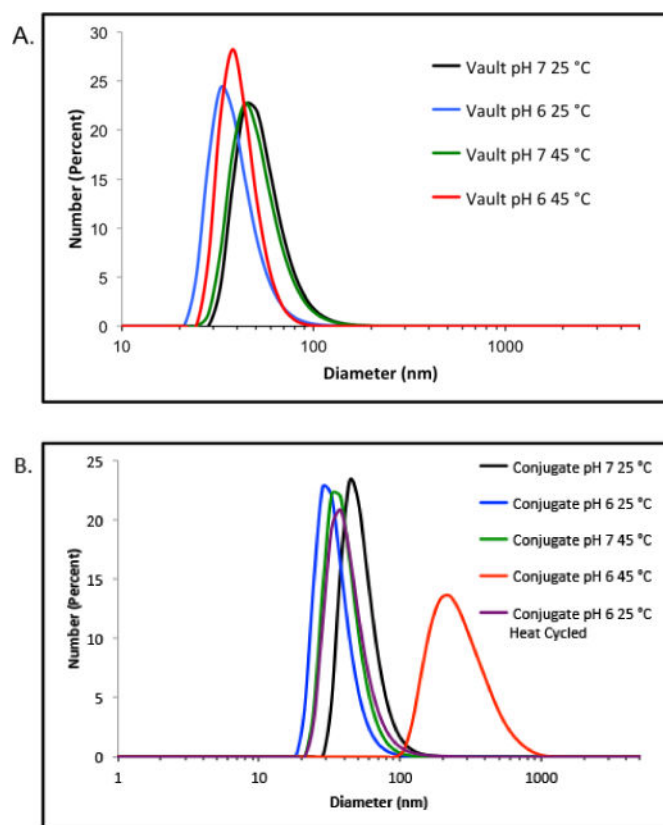


**Figure 2.** SDS-PAGE of hMVP vault and conjugate visualized by coomassie blue staining (Lane 1: protein marker; Lane 2: hMVP vault reducing conditions; Lane 3: conjugate reducing conditions; Lane 4: hMVP vault non-reducing conditions; Lane 5: conjugate non-reducing conditions).

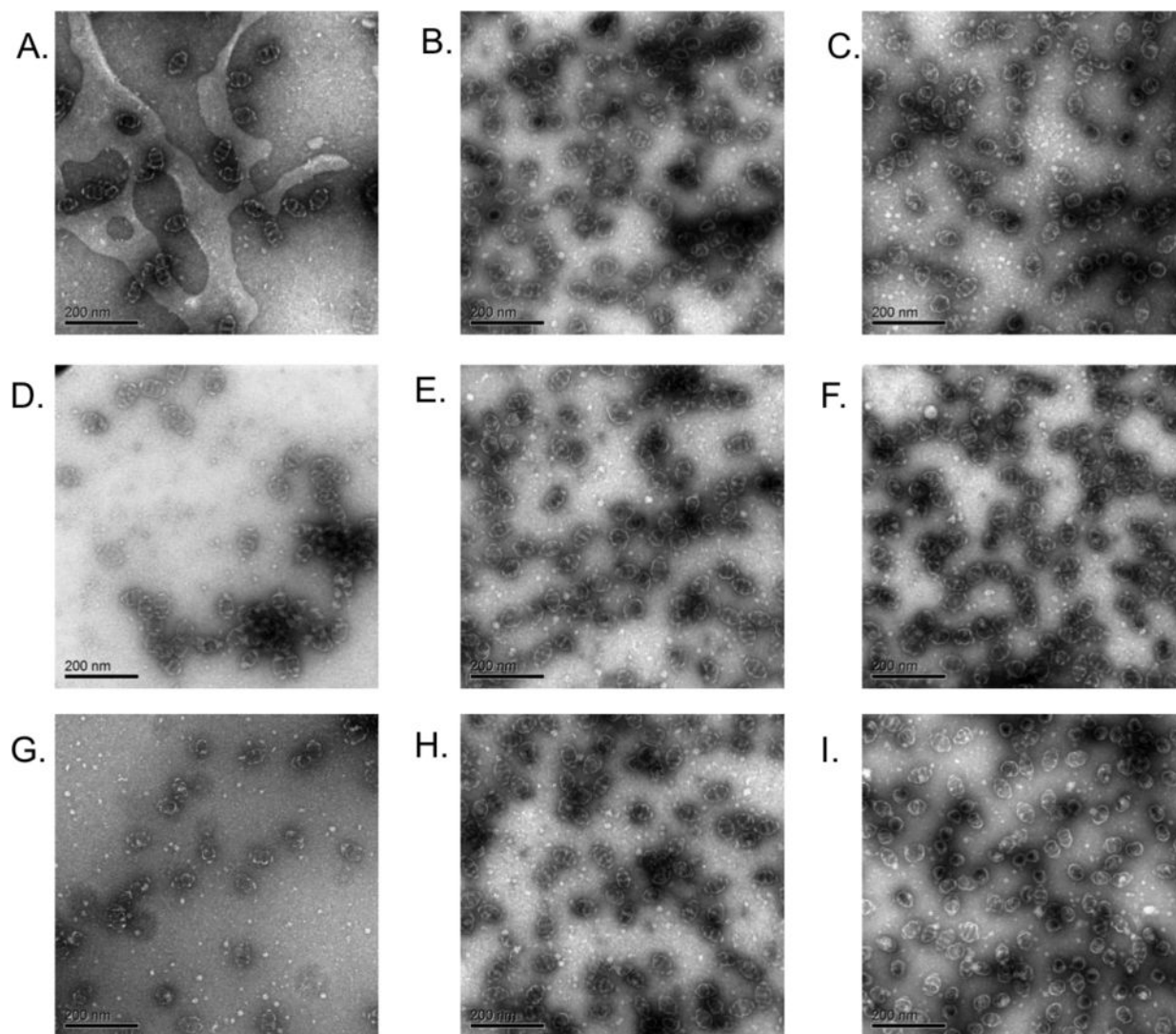


**Figure 3.**

UV-Vis turbidity experiments of the hMVP vault in 20 mM MES at: (A) pH 7.0 and (B) pH 6.0 and of the pNIPAAm-co-AA-hMVP vault conjugate at (C) pH 7.0 and (D) pH 6.0.

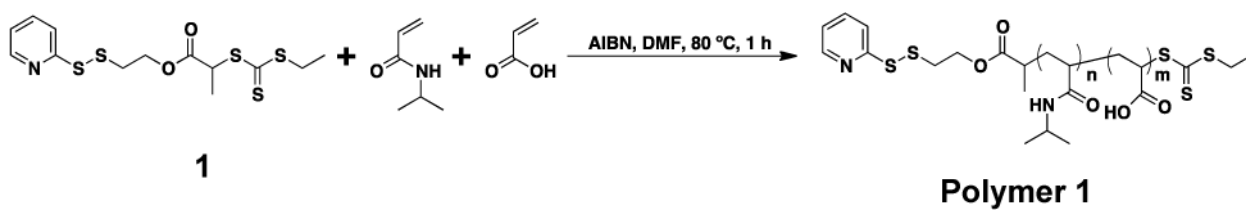


**Figure 4.** DLS measurements of: (A.) hMVP vaults; (B.) pNIPAAm-co-AA vault conjugates.

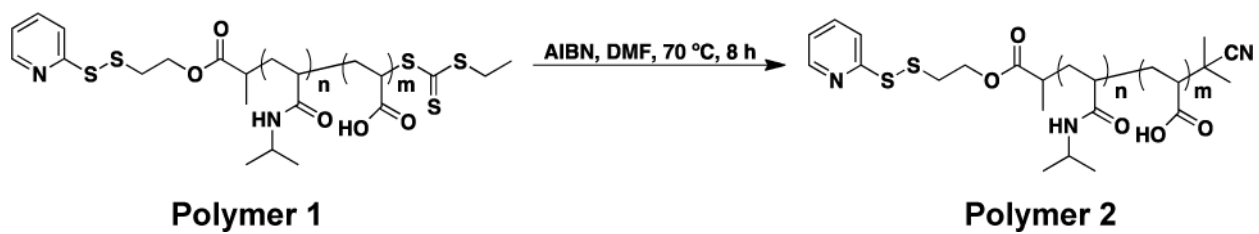


**Figure 5.** Negative stain TEM of (A.) hMVP vaults, pH 6.5, 4 °C; (B.) Conjugate pH 7.0, 4 °C; (C.) Conjugate pH 6.0, 4 °C; (D.) hMVP vaults heat cycled once (4 to 45 to 4 °C); (E.) Conjugate pH 7.0 heat cycled once (4 to 45 to 4 °C); (F.) Conjugate pH 6.0 heat cycled once (4 to 45 to 4 °C); (G.) hMVP vaults heat cycled three times; (H.) Conjugate pH 7.0 heat cycled three times; (I.) Conjugate pH 6.0 heat cycled three times.

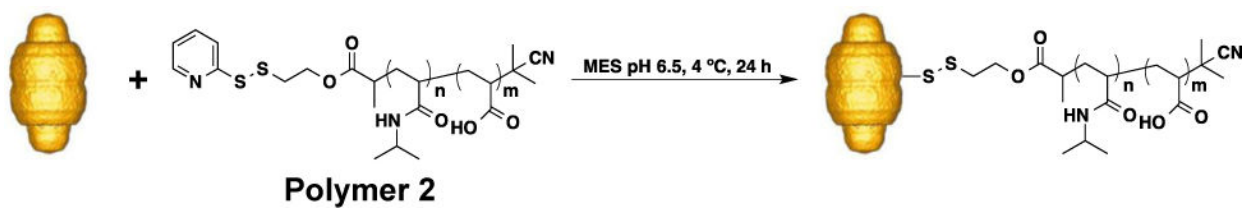




**Scheme 1.**  
RAFT copolymerization of NIPAAm and AA to yield **polymer 1**

**Scheme 2.**

Endgroup modification of **polymer 1** by radical exchange with AIBN to yield **polymer 2**.



**Scheme 3.**  
Conjugation of **Polymer 2** to hMVP Vaults